Received: 21 March 2021 | Revised: 26 May 2021 | Accepted: 27 May 2021

DOI: 10.1002/cne.25197

RESEARCH ARTICLE

JCN RESEARCH IN SYSTEMS NEUROSCIENCE THE JOURNAL OF COMPARATIVE NEUROLOGY WILEY

Cytoarchitectural characteristics associated with cognitive flexibility in raccoons

Joanna Jacob[1] | Molly Kent[2] | Sarah Benson-Amram[3,4] | Suzana Herculano-Houzel[5] | Mary Ann Raghanti[6] | Emily Ploppert[1] | Jack Drake[1] | Bilal Hindi[1] | Nick R. Natale[1] | Sarah Daniels[7] | Rachel Fanelli[7] | Anderson Miller[5] | Tim Landis[8] | Amy Gilbert[9] | Shylo Johnson[9] | Annie Lai[1] | Molly Hyer[8] | Amanda Rzucidlo[10] | Chris Anchor[10] | Stan Gehrt[11] | Kelly Lambert[1]

[1]Department of Psychology, University of Richmond, Richmond, Virginia

[2]Department of Biology, Virginia Military Institute, Lexington, Virginia

[3]Department of Forest and Conservation Sciences, University of British Columbia, Vancouver, British Columbia, Canada

[4]Department of Zoology and Biodiversity Research Center, University of British Columbia, Vancouver, British Columbia, Canada

[5]Department of Psychology, Vanderbilt University, Nashville, Tennessee

[6]Department of Anthropology, School of Biomedical Sciences, and Brain Health Research Institute, Kent State University, Kent, Ohio

[7]Department of Zoology and Physiology, University of Wyoming, Laramie, Wyoming

[8]Department of Psychology, Randolph-Macon College, Ashland, Virginia

[9]USDA-APHIS-WS National Wildlife Research Center, Fort Collins, Colorado

[10]Forest Preserve District of Cook County, River Forest, Illinois

[11]School of Environment and Natural Resources, Ohio State University, Columbus, Ohio

Correspondence
Kelly Lambert, Department of Psychology, University of Richmond, VA 23173, USA.
Email: klambert@richmond.edu

Abstract

With rates of psychiatric illnesses such as depression continuing to rise, additional preclinical models are needed to facilitate translational neuroscience research. In the current study, the raccoon (*Procyon lotor*) was investigated due to its similarities with primate brains, including comparable proportional neuronal densities, cortical magnification of the forepaw area, and cortical gyrification. Specifically, we report on the cytoarchitectural characteristics of raccoons profiled as high, intermediate, or low solvers in a multiaccess problem-solving task. Isotropic fractionation indicated that high-solvers had significantly more cells in the hippocampus (HC) than the other solving groups; further, a nonsignificant trend suggested that this increase in cell profile density was due to increased nonneuronal (e.g., glial) cells. Group differences were not observed in the cellular density of the somatosensory cortex. Thionin-based staining confirmed the presence of von Economo neurons (VENs) in the frontoinsular cortex, although no impact of solving ability on VEN cell profile density levels was observed. Elongated fusiform cells were quantified in the HC dentate gyrus where high-solvers were observed to have higher levels of this cell type than the other solving groups. In sum, the current findings suggest that varying cytoarchitectural phenotypes contribute to cognitive flexibility. Additional research is necessary to determine the translational value of cytoarchitectural distribution patterns on adaptive behavioral outcomes associated with cognitive performance and mental health.

KEYWORDS
cognitive flexibility, cytoarchitecture, raccoon, von Economo neurons

1 | INTRODUCTION

Given the current challenges associated with the identification of appropriate preclinical models for psychiatric illnesses (Denayer et al., 2014), the raccoon (*Procyon lotor*), a species virtually ubiquitous in North America, offers potential as an informative translational model for primate brains (Hamir, 2011). Specifically, primates and raccoons share similar cortical neuron density profiles, a high

degree of cortical gyrification, and corresponding cortical magnification of forepaw/hand areas (Jardim-Messeder et al., 2017; Krubitzer, 2007; Pubols et al., 1965). Anecdotally known for their intelligence and advanced problem-solving abilities (Zeveloff, 2002), raccoons appear to also share behavioral and cognitive characteristics such as cognitive flexibility with humans and other primates. Their behavioral adaptability is evident by their infiltration of a wide variety of habitats including areas with vastly different temperature ranges, levels of urbanization, vegetation, and elevation (Gienapp et al., 2008).

Although the natural history, anatomy, and roles of disease transmission of the Northern raccoon have been thoroughly investigated (Hirsch et al., 2013; Iwaniuk & Whishaw, 1999; MacClintock, 2002; Prange et al., 2004), few studies have systematically explored cognitive and behavioral strategies in these animals. Early 20th century studies patterned after experimental psychologist Edward Thorndike's puzzle box approach suggested that raccoons were curious and innovative, with their putative intelligence level on a "higher-order" than cats and dogs and more in line with nonhuman primates (Cole, 1907; Davis, 1907). Subsequent research provided evidence that raccoons retained information in a delayed reaction task more efficiently than dogs and rats (Hunter, 1913; Hunter, 1915). After this time, however, rats ascended to the research scene in psychology laboratories, as well as other biomedical laboratories, diminishing interest in the raccoon as a viable research model for cognitive functions (Lambert et al., 2019; Pettit, 2010). After nearly a century-long hiatus from research focused on raccoon cognition and neurobiological functions, more recent studies have corroborated earlier conclusions about their unique problem-solving abilities. Specifically, when presented with an Aesop's Fable type of task designed to assess an understanding of water displacement, raccoons used innovative approaches to solving the task such as using their bodies to upend the apparatus as opposed to the more predictable strategy of adjusting the water level with strategic pebble placement (Stanton et al., 2020). When exposed to multi-access puzzle boxes similar to the initial laboratory problem-solving assessments of raccoons, both success and innovation were observed, as well as pronounced individual differences (Daniels et al., 2019). Cognitive flexibility of raccoons was recently assessed in a reversal-learning task and the animals exhibited rapid associative learning by successfully completing reversals with observed trends in improvement over time (Stanton et al., 2020). Interestingly, in a task requiring the use of a stick to push desired food through a pipe, wild raccoons exhibited a dependence on olfaction and somatosensory exploration instead of manipulating the stick to obtain the food reward (Morton, 2020).

A potential underlying neural mechanism of the observed cognitive efficacy of raccoons in natural habitats is the presence and distribution of von Economo neurons (VENs). Although previously described by neuroanatomists including Santiago Ramón y Cajal, Constantin von Economo provided a thorough description of these rod and corkscrew-shaped neurons and their typical locations in anterior cingulate and frontoinsular (FI) cortical areas (von Economo, 1926; as described in Allman et al., 2010). Subsequent computer-assisted and immunohistological analyses confirmed these distinctive cell types in Layer Vb of the human anterior cingulate cortex (Nimchinsky et al., 1995). Initial comparative analyses suggested that the cells were unique to humans and great apes, with higher VEN densities in human primates (Allman et al., 2011; Nimchinsky et al., 1999). Subsequent research, however, has confirmed the presence of VENs in other mammalian species including cows, sheep, deer, horses, pigs, Nile hippopotami, elephants, macaques, and whales (Butti et al., 2013; Butti et al., 2014; Butti et al., 2015; Evrard et al., 2012; Hakeem et al., 2009; Hof & Van Der Gucht, 2007; Raghanti et al., 2015; Raghanti et al., 2019), as well as in avian species (i.e., parrots (Shubha & Suchi, 2017)). It has been proposed that the VENs arose independently in cetaceans, elephants, and hominids and may be necessary to overcome the geometric challenges associated with rapid neural processing in large brains, especially considering that VENs are not reliably present in the elephant's closest living relative that is comparatively much smaller, the rock hyrax (Hakeem et al., 2009; Raghanti et al., 2015).

Characterized as fast projecting cells, VENs in the insular area are speculated to be associated with interoception, emotional processing, and task-directed responses (Seeley et al., 2006; Ibegbu et al., 2015). Hominoid VENs exhibit immunoreactivity to proteins such as interleukin 4 receptor, neuromedin B, and activating-transcription factor 3 (Sherwood et al., 2006; Stimpson et al., 2011). In unpublished findings in our laboratory, a stereological investigation of three wild adult raccoon brains confirmed the presence of VENs in the FI (see Figure 1). The percentage of VENs in raccoons was observed to be approximately 6% of the neuronal cellular population, compared to previously reported 11% in the human anterior insular cortex and 8 and 5% in the cow and horse, respectively (Raghanti et al., 2015). In this initial unpublished analysis, VENs were not observed in the raccoon ACC as they have been observed in other species, a finding that deserves further investigation.

Morphologically, VENs are defined by their thin, elongated cell body and long dendrites projecting from apical and basal neural processes (Correa-Júnior et al., 2020). They are often found in proximity to large neurons with a bifurcated apical dendrite known as fork cells (Dijkstra et al., 2018; Raghanti et al., 2015). Once thought to be specific to large-brained animals exhibiting complex social-cognitive behavior (e.g., hominoid primates and cetaceans), as previously mentioned, VENs have been observed in perissodactyls, artiodactyls, afrotherians, and other primates (Raghanti et al., 2015). Although the existence of VENs in such diverse species supports the suggestion that VENs are the result of convergent evolutionary processes facilitating varying adaptive specializations, it is also a possibility that VENs are associated with the mechanical challenges associated with larger, gyrencephalic brains. Consequently, more research is necessary to elucidate evolutionary adaptations associated with these neurons.

Another likely neuroanatomical determinant of problem-solving abilities of raccoons is the neurophysiological processing of the hippocampus (HC), a brain structure known for its role in cognitive and emotional processing (Bird & Burgess, 2008; Hartley et al., 2007;

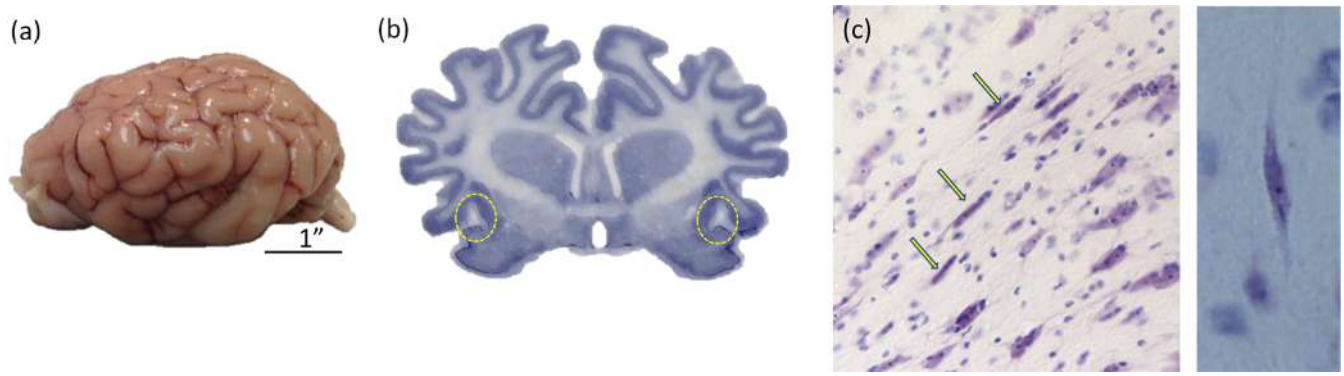

FIGURE 1 Representative images of neuroanatomical characteristics in the raccoon. Cortical gyrification is observed in the intact raccoon brain (a) and in an anterior coronal thionin-stained section, the frontoinsula region (b) is identified (dashed circles). A few representative von Economo neurons are identified in the frontoinsular cortical region (c) at 5× (left) 40× (right) magnification [Color figure can be viewed at wileyonlinelibrary.com]

Maguire et al., 2003; Tyng et al., 2017). Activation of the HC in humans, especially in the right hemisphere, has been implicated in insight learning related to unique problem-solving tasks (Luo & Niki, 2003). Hippocampal volume has been associated with enhanced spatial abilities related to foraging in rodents, caching and spatial memory in birds, and navigational skills in London taxi drivers (Krebs et al., 1989; Pravosudov & Clayton, 2002; Maguire et al., 2006). Also critical for learning processes, the HC serves as a hub for neuroplasticity with neural circuits exhibiting the ability to modify functional capabilities quite rapidly for long-term periods (Lynch et al., 1978). The dentate gyrus, embedded in the HC, is recognized as a neurogenic zone, producing new neurons throughout an animal's life (Kempermann and Gage, 1999; Kempermann, 2002) that contribute to the malleability of the brain's synaptic wiring and functional adaptations (Citri et al., 2008). Within the dentate gyrus, the hilar area has been associated with the identification of relevant changes in external stimuli (i.e., pattern separation), an important element of effective cognitive strategies (Myers & Scharfman, 2009; Yassa & Stark, 2011).

The distributions of different cellular phenotypes within the cortex and HC (e.g., percentages of various glial and neuronal cells) may also be important contributors to cognitive abilities (Dallérac & Rouach, 2016). Glial to neuronal ratios, for example, have been explored across species with interesting results suggesting that increased glial cell densities do not appear to be dependent on increased metabolic needs for neurons (Herculano-Houzel, 2011; Herculano-Houzel, 2014), opening the possibility for alternative interpretations such as an impact on synaptic processes or cognitive abilities (Vasile et al., 2017). In primate investigations, humans have been shown to have higher glial to neuron ratios in the dorsolateral prefrontal cortex compared to 18 species of anthropoids (Sherwood et al., 2006). Focusing on astrocytes' influence on neuronal functions, these specific glial cells are known to fully participate in neural processes and have been implicated in facilitating the integration of neural networks (Poskanzer & Yuste, 2016; Santello et al., 2019). Thus, the distribution of specific cellular phenotypes may translate to neural efficiency and cognitive variations.

In the current study, we explored potential neuroanatomical determinants of problem-solving ability in wild-caught, captive raccoons assessed behaviorally in a previously published study (see Daniels et al., 2019). After the animals were profiled into high, intermediate, and low problem-solving ability categories, the number of neural cells (neurons and nonneurons) in the HC and somatosensory cortex (SSCX; a cortical area associated with forepaw use in the raccoon; Krubitzer, 2007) was determined using isotropic fractionation (IF; Herculano-Houzel & Lent, 2005). Further, to determine cellular phenotypes in the HC and FI cortex, thionin-based histological assessments were conducted to determine the presence of VENs and non-VENs (i.e., glial cells and other neurons) in the FI cortex for the three groups of animals. It was hypothesized that high-performing raccoons would have altered distributions of hippocampal cells, as well as a higher number of VENs in the FI cortex, than the other groups. Although the SSCX was hypothesized to play an integral role in interacting with the task, this area was not hypothesized to be directly implicated in cognitive flexibility; consequently, no cellular differences were hypothesized across the problem-solving groups.

2 | MATERIALS AND METHODS

2.1 | Animals

Eighteen wild raccoons (*P. lotor*) were live-trapped in Larimer County, CO, near the National Wildlife Research Center (NWRC). The animals were maintained in captivity for up to 2 years prior to behavioral assessments. One female gave birth while housed at the NWRC. Two of the offspring were included in the behavioral study, bringing the subject total to 20 raccoons (male $N = 8$; female $N = 12$; estimated average age = 2.9 years, estimated age range 2–5 years). All raccoons were individually housed in an outdoor enclosure (3 × 3 × 2.5 m).

The study was approved by the Animal Review Board at the USDA NWRC (QA-2492).

As described in a previous publication (Daniels et al., 2019), these animals were assessed for cognitive flexibility using a multiaccess problem-solving box prior to the histological analysis in the current study to explore neural contributions to problem-solving abilities in this species Briefly, each raccoon was presented with a puzzle box apparatus containing a food reward (see Figure 2 for graphic description of this task). The puzzle box could be opened via three solution types: a window, a side latch, and a door. To move forward in the trials, the animal had to successfully open a solution type and retrieve the reward three times. Raccoons that failed to do so were recorded as *nonsolvers* ($n = 6$) and further testing ceased. Raccoons that successfully solved the same solution three times were tested on subsequent nights, with the initial preferred access method locked. The puzzle box was presented again but with only two remaining solution types unlocked and available. The same procedure was followed where animals needed to solve one of the remaining solution types at least three times to move on to the next night of testing. On the third and final night of testing, successful individuals were presented with the puzzle box with the two previously opened solution types locked and one remaining solution type unlocked and available. Those raccoons that solved one or two solution types were labeled *intermediate solvers* ($n = 5$). In this study, there were no raccoons that only solved one solution type, so all of the intermediate solvers opened two solution types. Finally, the raccoons that successfully solved all three solution types three times each were labeled *high-solvers* ($n = 7$), as they were representative of the most cognitively flexible animals. Due to tissue loss in the preparation and processing of the brains, two were not suitable for further processing, leading to lower numbers than used for the behavioral assessment. As previously mentioned, the full behavioral results are reported as a separate manuscript (see Daniels et al., 2019). Following the completion of additional in vivo studies approved at the NWRC and at the time of tissue sampling for those studies, the animals were humanely euthanized by inducing anesthesia with 5% isoflurane at 5 L/min, followed by an intermuscular injection

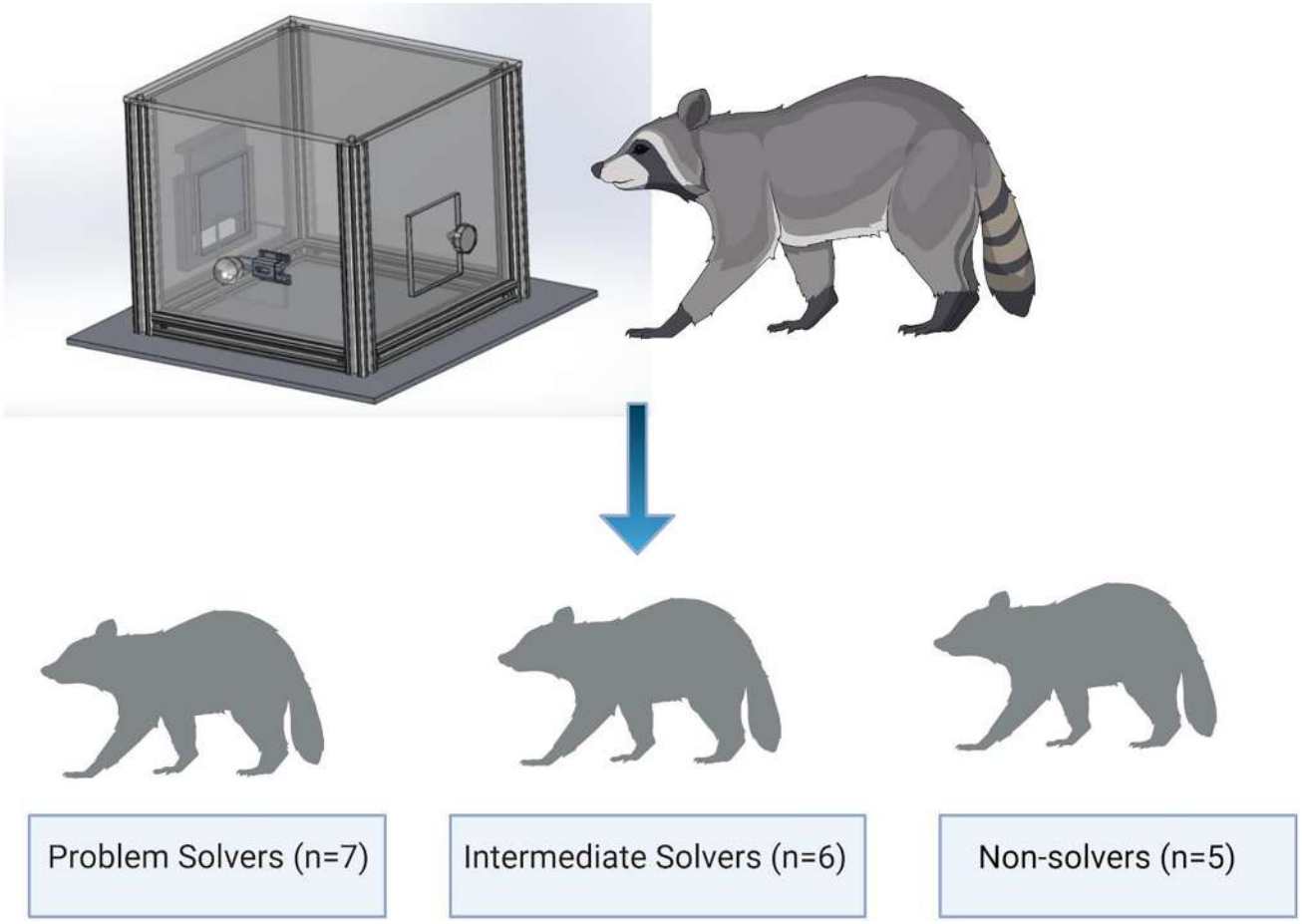

FIGURE 2 Representation of the puzzle box behavioral task to assess cognitive flexibility. Raccoons were introduced to the puzzle box apparatus containing a food reward inside, obscured by three different locking mechanisms, each one outfitted on a different access window. After raccoons demonstrated they could obtain the reward via one locking mechanism on three independent trials, the initial locking option was locked to force the animal to solve a second locking mechanism, and subsequently, a third locking mechanism. *Nonsolvers* included animals that did not successfully access the reward through any of the available windows on first exposure, and were not allowed to advance in the task. *Intermediates* included animals that solved up to two of the three access mechanisms correctly, and *solvers* (also referred to as high-solvers) included animals that successfully opened all three locking mechanisms, three times each (see Daniels et al., 2019) [Color figure can be viewed at wileyonlinelibrary.com]

of ketamine-xylazine mix (10 mg/kg ketamine [100 mg/ml, Zetamine, VetOne, Boise, Idaho] and 2 mg/kg xylazine [100 mg/ml, XylaMed, VetOne]) and then a 2–4 ml cardiac injection of pentobarbital and phenytoin sodium (Euthanasia Solution, VetOne).

2.2 | General histological procedures

Intact brains postfixed in 4% paraformaldehyde were received in our laboratory and stored at 4°C. Once the brains were weighed, the dura mater was removed so they could be separated along the longitudinal fissure into the left and right hemispheres that were subsequently weighed once again. The right hemisphere was assigned to IF analyses and the left hemisphere to thionin-based histological analyses. In a few cases, however, the right cortical tissue was slightly compromised with an occasional nick in the cortex, making it inappropriate for IF histology; in those cases, the left hemisphere was assigned to the IF group. For cryoprotection prior to sectioning, the hemispheres dedicated to thionin-based histology were transferred to a series of 10, 20, and 30% sucrose solutions, with 1 week between each interval. The remaining hemisphere was maintained in 4% paraformaldehyde and was further dissected and processed regionally for IF assessment. All ingredients of the fixative solution were purchased from Sigma Aldrich, St. Louis, MO. The brains were coded to ensure experimenters were blind to the animal's group assignment based on the behavioral task described above.

2.3 | IF histological procedures

The HC and SSCX from one hemisphere of each brain were carefully dissected from the tissue and processed for IF, a method used to determine cell density of specific brain areas (Herculano-Houzel & Lent, 2005). For each dissected hemisphere, half of the HC was removed in its entirety in the curved bean-shaped form of the hippocampal formation (CA fields and dentate gyrus), encapsulated in white matter. The SSCX for that same hemisphere was collected by removing the entirety of the subcortical white and gray matter by peeling the cortex from the striatum (Bandeira et al., 2009). Specifically, the SSCX was defined as the cortical area caudal to the sulcus cruciatus, anterior to the sulcus ansatus, and dorsal to the sulcus sylvius (Herron, 1978; Krubitzer & Dooley, 2013; Schober, 1991; Welker & Seidenstein, 1959). Each targeted region was weighed (see Table 1 for brain section weights for each group), then the entire dissected region of interest (ROI) was sectioned into small pieces of tissue comprised of all gray and white matter and placed in a handheld glass Dounce 40 ml homogenizer (Kontes Glass Co., Vineland, NJ). A minimum of 1 ml chilled dissociation solution (40 mM sodium citrate and 1% Triton-X100; Sigma Aldrich) per 100 mg of tissue was utilized for the mechanical disruption process. Tissue pieces were ground until no longer visible, adding dissociation solution as needed, to ensure that a sufficient nuclei suspension had been obtained. Following homogenization, the suspension was poured into a graduated cylinder where the fluorescent marker, 4,6-diamidino-2-phenylindole dihydrochloride (DAPI; Sigma Aldrich) (10 mg/ml), was added to visualize cell nuclei. The final volume was recorded before the homogenates were transferred to a new conical tube, which was stored at 4°C and protected from light. Because the brain sections were removed in their entirety, including gray and white matter, cellular numbers were expected to be higher than previous reports exclusively using gray matter.

To count total nuclei, 1 ml aliquots were homogenized using a handheld cordless Bel-Art homogenizer and a clean plastic pestle (Cole-Parmer, Vernon Hills, IL). A total of 10 μl was loaded onto a Neubauer chamber (i.e., hemocytometer) and placed under a *Zeiss Axio* microscope for visualization. Nuclei were initially visualized under the DAPI filter at 10× magnification for proper positioning, before moving to 40× for counting. Utilizing the centered 1 × 1 mm^2 square etched into the hemocytometer as the counting field, experimenters selected 10 of the 25 squares along an "X" pattern, summing the number of nuclei present in each small square, which each held a volume of 4 nl (Figure 3(b)). To obtain a representative sample count, this process was repeated four times. The cell counts were summed, averaged, and a coefficient of variation was calculated, which had to be lower than the 15% predetermined criterion to be acceptable. The following equation was utilized to calculate the total nuclei present in the original sample and, subsequently, extrapolate the cell count for the particular ROI from each animal:

$$\text{Average nuclei count} \times (1{,}000{,}000/\text{volume [nl] counted}) \times \text{total sample volume (ml)}$$

Since the initial counts consisted only of DAPI-positive nuclei, a fluorescent molecule that binds to DNA regions rich with adenine-thymine interactions, there was no molecular differentiation between neurons and nonneurons at this stage. To evaluate the neuronal percentage present in each sample, an aliquot (1 ml) of homogenates for each animal and ROI was co-stained for the neuronal nuclear protein marker, NeuN, using a Cy3 labeled primary anti-NeuN

TABLE 1 Hemisphere and brain area weights

Solver type	Hemisphere weight (g)	Hippocampus (mg)	Somatosensory cortex (g)
Nonsolver ($N = 6$)	19.18 ± 0.99	381.39 ± 100.87	5.32 ± 0.55[a]
Intermediate ($N = 5$)	19.16 ± 0.82	473.60 ± 120.99	4.56 ± 0.46
Solver ($N = 7$)	18.52 ± 0.82[a]	553.69 ± 116.48	5.22 ± 0.13[a]

Note: Values represent averages ± *SEM*.
[a]*N* - 1, value missing for one animal.

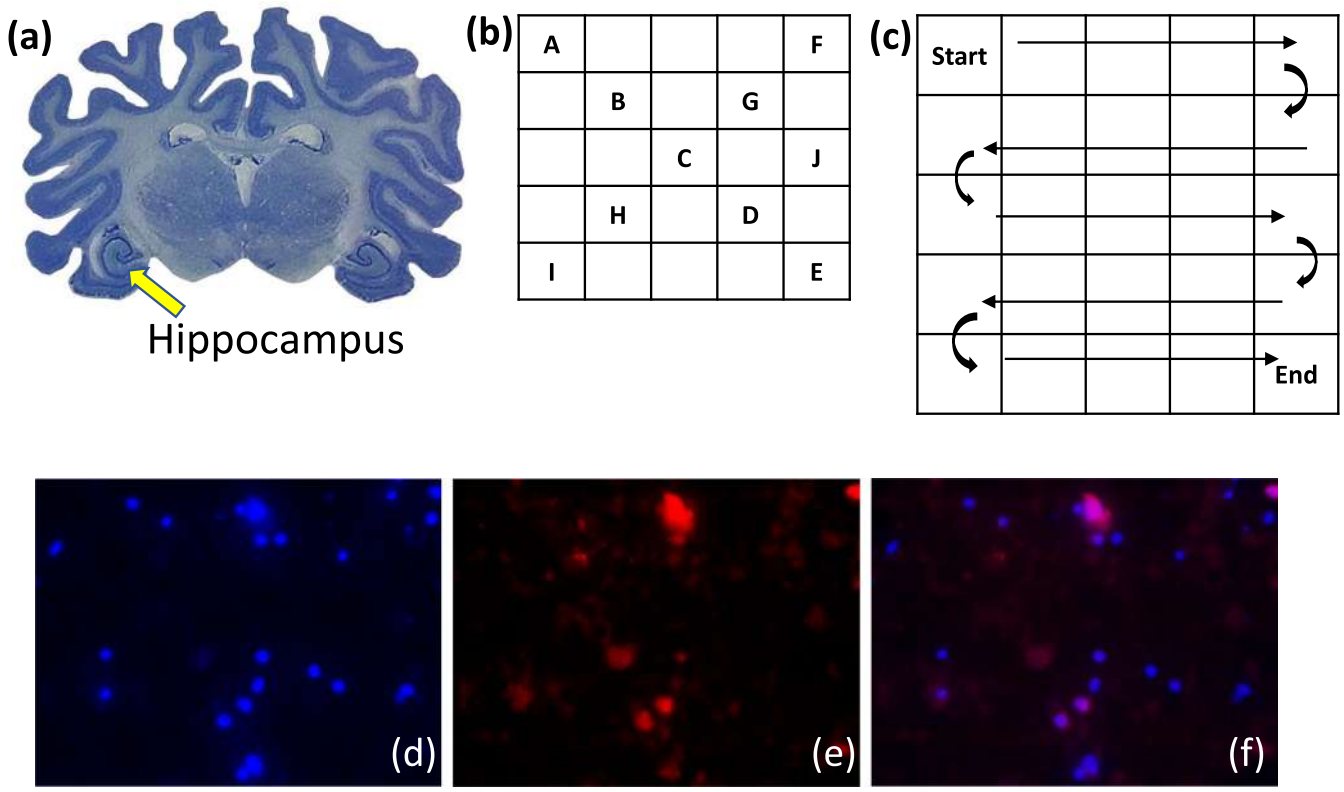

FIGURE 3 Isotropic fractionation. The somatosensory cortex (not shown) and hippocampus (a) were dissected from one hemisphere and evaluated for cellular density using isotropic fractionation. Cells were stained with DAPI to visualize individual nuclei, then loaded onto a hemocytometer and counted in an X pattern (b) under a light microscope to determine cell densities. Following 4,6-diamidino-2-phenylindole dihydrochloride (DAPI) counting, the cell homogenates were treated with anti-NeuN and visualized at 40×, again on a hemocytometer, where all cells in the 25 × 25 grid pattern were counted (c) and characterized as neuronal or nonneuronal. Cells visible under the DAPI channel (d) that were also visible under the TRITC channel (e) were determined to be neurons, further confirmed by the merged image showing colocalization (f). Cells that were only visible under the DAPI channel were characterized as nonneuronal [Color figure can be viewed at wileyonlinelibrary.com]

antibody, ABN78C3 [1:300] (Millipore Sigma, Burlington, MA). The aliquots were processed initially with an antigen-retrieval step (1 h at 75°C in 0.2 M boric acid, pH 9) to improve access to available binding sites. Following the antigen retrieval step, the samples were stained with anti-NeuN in PBS-BSA (5%) and incubated for 24–48 h at 4°C, protected from light. The stained homogenates were then collected in a tabletop centrifuge (5 min, 1500*g*), the supernatant was decanted, and the sample pellet was resuspended in up to 1 ml PBS and protected from light with foil.

To determine the neuronal percentage, 10 μl samples were loaded onto the hemocytometer and 100 nl volumes were counted until a minimum of 500 cells were identified under the DAPI filter (Figure 3(c)). Cy3 fluorescence (~550 nm excitation, ~570 nm emission) was visualized under the standard TRITC filter. Photomicrographs of cell nuclei were captured under each filter to assess those that exhibited DAPI only, or DAPI and NeuN staining, using the Zeiss Zen software. Cell counts were determined by observers who were blind to group conditions; further, an interobserver reliability agreement threshold of 90% was established prior to cell quantification to assure that variation among observers did not exceed 10%. The number of co-stained nuclei was divided by the total number of DAPI-stained nuclei, and multiplied by 100 to determine the percent of neurons in the sample. See Figure 3 for IF procedures.

2.4 | Thionin-staining histological procedures

The FI cortex and the ventral HC from one hemisphere of each raccoon brain were processed for morphological cellular analysis using thionin-stained sections. Because the anterior portion of the HC has a large ventral presence, similar to humans and foxes, thought to be due to the increased neocortical tissue (Kempermann, 2012), the ventral hippocampal area was investigated in the current study. Each hemisphere was cryopreserved by transferring the tissue into 20% and then 30% sucrose prior to sectioning; subsequently, the tissue was blocked in appropriate sections to reveal the FI in one section and, more posterior, the HC section. Segments were mounted using Fisher Healthcare Tissue Plus O.C.T compound (Wilmington, MA), and placed in an M525 Microm microtome cryostat (Thermo Fisher Scientific) at −20°C for 20 min, or until fully frozen, prior to sectioning. The tissue was then sectioned at a thickness of 50 μm, thaw-mounted

onto charged microscope slides (2 × 3 in) (Thermo Fisher Scientific), and allowed to dry for 48 h before staining with thionin (0.1% dilution) (Allied Chemical Corporation, Morristown, NJ) and coverslipping with permount (Electron Microscopy Sciences, Hatfield, PA). To generate average cell profile density measures for individual sampling areas, an average of three sections was quantified per animal for the HC samples. For the FI analysis, an average of nine brain sections was quantified per animal. The comparatively low number of HC sections was due to more frequent tissue damage in this area compared to the FI sections, likely due to the postfixed, rather than perfused, tissue used in this study. Tissue was imaged on a Zeiss Axioscope *M.2* light microscope (Carl Zeiss, Oberkochen, Germany) equipped with Neurolucida software version 2020 3.1 (Microbrightfield, Inc., Williston, VT). The area of interest (either dentate gyrus of the HC or FI cortex) was first visualized at 5× magnification and, using consistent visual landmarks, each area was marked with three (HC) or four (Layer V FI) computer-generated markers to identify the specific counting locations within each region (see Figure 5). Once the targeted area was identified at low magnification to assure consistent placement of the software generated reference marker, the objective was then moved to 40× magnification for quantification within a 200 × 300 μm^2 perimeter box. All visible neurons and glial cells were quantified using this two-dimensional (2D) assessment. Considering the relatively large sampling window, consistent sampling locations, interobserver reliability agreement thresholds set at 90%, and the ample distance between sections (150 μm) to avoid double counting cells, the 2D use of the x and y planes was determined to be appropriate to generate accurate estimates (Benes & Lange, 2001). In the FI, neurons were categorized as VENs, (defined as an elongated bipolar cell body), forked cell (large cell body with bifurcating apical dendrite), or non-VENs (e.g., pyramidal cells); glial cells were categorized using criteria previously outlined (see Garcia-Cabezas et al., 2016). In the HC, the same categories were used with the exception of the VEN category. Since to our knowledge VENs have not been identified in the HC of any species, fusiform cells were assessed due to their similar elongated phenotype as observed in the VENs (Dickerson et al., 2007; Schwerdtfeger & Buhl, 1986). Within each thionin-stained section, average cell profile density levels were obtained by counting three ROI perimeter boxes per HC tissue section and four ROI boxes for each FI tissue section. The average density counts for each ROI box in the targeted brain area was determined for each solving group and subsequently used for further data analyses. See Figure 5 for consistent placement of sampling boxes for the thionin quantification procedures.

2.5 | Statistical methods

In all comparisons of the three solving groups, data were assessed via one-way analysis of variance (ANOVA) assessments determining the effects of three levels of task performance ability on the various cytoarchitectural measures in SPSS Statistics software, version 27. When appropriate, Tukey's post hoc tests were performed to detect group differences (with an alpha value of .05). One histology assessment did not include intermediate solvers due to tissue loss; in that case, the two remaining groups were compared using Student's two-tailed *t* test, with an alpha value of .05. Descriptive statistics were calculated through SPSS or Excel. All data are shown as mean ± *SEM* for each group unless otherwise noted. Graphs and figures were generated using *GraphPad Prism* software, version 6.0 and BioRender.com, respectively.

3 | RESULTS

3.1 | IF-determined cell density

Based on prior evidence that raccoons exhibit cortical magnification of their forepaw/hand areas, we investigated the SSCX since it is an area essential to interactions with physical stimuli but was not expected to impact cognitive functions. High-solvers ($x\bar{c}$ = 270,594,097) did not differ from either intermediate solvers ($x\bar{c}$ = 214,821,875) or nonsolvers ($x\bar{c}$ = 242,337,500) in total nuclei. Further, intermediates and nonsolvers were also not found to differ from one another. Although no effect of task performance was observed for total cell density in the SSCX, a significant overall effect was observed for the total HC nuclei and total nonneuronal HC nuclei ($F(2,15) = 6.067$, $p = .0117$, $\eta_p^2 = 0.447$; $F(2,14) = 3.847$, $p = .0466$, $\eta_p^2 = 0.355$, respectively). Post hoc tests indicated that the high solvers had significantly more cells ($x\bar{c}$ = 51,472,917) than the nonsolver group ($x\bar{c}$ = 35,237,500; $p = .012$; see Figure 4(a)). A similar trend was observed for total cell count between high solvers and the intermediate group ($x\bar{c}$ = 39,017,500), but did not reach statistical significance ($p = .0663$). Additionally, high solvers were found to have more nonneuronal nuclei on average ($x\bar{c}$ = 43,959, 439) compared to nonsolvers ($x\bar{c}$ = 31,523, 979) and intermediates ($x\bar{c}$ = 32,545,144); however, this observation is most accurately described as a nonsignificant trend since the post hoc tests failed to reach a statistically significant threshold for either comparison ($p = .071$ and $p = .101$, respectively; see Figure 4(b)). One intermediate solver could not be analyzed for NeuN staining due to poor sample quality. No group differences in NeuN+ cells were observed.

For additional characterization of the brain areas used for the IF analyses, a one-way ANOVA was used to determine differences among hemisphere, HC, and somatosensory cortical weights. No statistical differences were observed in these measures (see Table 1 for group means for each brain area).

3.2 | Morphology-based cellular categories in dentate gyrus and FI cortex

IF provides an accurate assessment of total regional cell counts, but it does not provide specific information about morphological characteristics

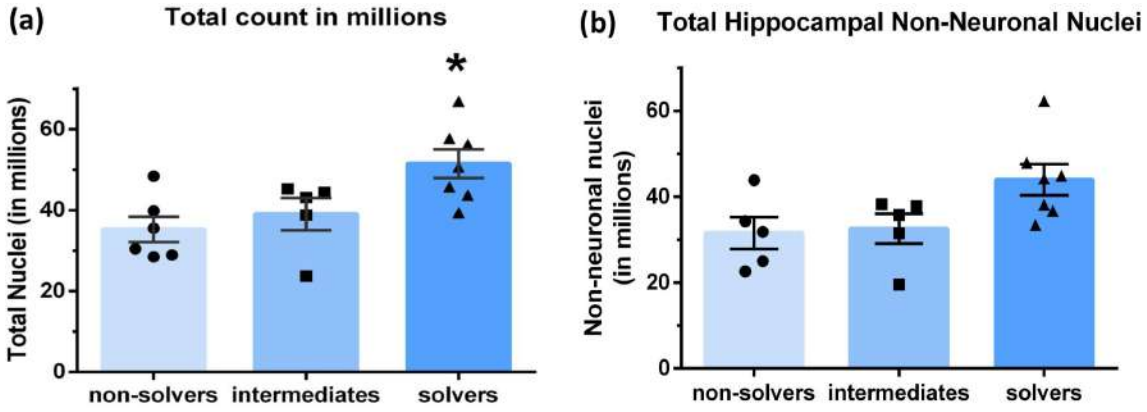

FIGURE 4 Isotropic fractionation-based cellular profiles in the raccoon hippocampus. (a) High-problem solving raccoons ($N = 7$) were found to have significantly higher total cell counts (i.e., nuclei) in the hippocampus compared to nonsolvers ($N = 6$) (*$p = .0117$) as determined by one-way analysis of variance (ANOVA) with Tukey's post hoc tests. (b) Isotropic homogenates stained with anti-NeuN revealed a greater proportion of nonneuronal cells present in high-problem solving raccoons following a one-way ANOVA ($p = .0466$), though post hoc tests failed to demonstrate significant group differences (solvers vs. nonsolvers: $p = .0706$; solvers vs. intermediates: $p = .1006$) [Color figure can be viewed at wileyonlinelibrary.com]

of the cellular components in the brain. As previously described, to further investigate the cellular phenotypic distribution in the brains of these raccoons, one hemisphere from each animal was devoted to cryopreservation and sections containing either the FI cortex or HC were assessed for the presence of neurons, nonneurons (i.e., glial cells), fork cells, or VENs (FI)/fusiform cells (DG; see Figure 5). Thionin-stained tissue containing the FI cortex was unavailable for intermediate solvers; therefore, group comparisons were between high solvers and nonsolvers only. In the FI cortex, high solvers had fewer average total cell density levels in the sampled visual fields; however, no statistically significant differences were observed compared to nonsolvers ($p = .2829$; see Table 2). Further, no significant differences were observed in nonneuron average counts ($p = .1503$; Welch's corrected t test used due to heterogeneity of variance for this measure). Fork neurons and von Economos were observed throughout the FI in all problem-solving types (see Figure 6), yet no differences in cell profile density levels were detected among groups for total VENs or fork neurons or for percentage levels of VENs or neurons ($p > .05$ in all comparisons; see Table 2). Although thionin-stained cell sampling via ROI cellular counts data fall short of the accuracy of a full stereological analysis, the percent of VENs observed in the sampled FI areas of these raccoons (approximately 8%) was higher, yet similar to the previous stereological assessment (6.33%) shown in Figure 1.

Cellular distribution was also assessed in the HC in thionin-stained sections; specifically, in the hilus of the dentate gyrus. Unlike the FI cortex, tissue was available for all three solving groups. Focusing on total neuron and nonneuron averages, high solvers did not differ significantly from either intermediates or nonsolvers; however, high solvers were found to contain higher numbers of fusiform-shaped neuronal cells ($x\bar{c} = 1.42$) in targeted sampled areas compared to intermediates ($x\bar{c} = 0.61$, $p = .0495$) and nearly significantly more than nonsolvers ($x\bar{c} = 0.79$, $p = .0692$; $F(2,11) = 4.640$, $p = .035$, $\eta_p^2 = 0.458$). See Figure 7 for graphs and representative photomicrographs and Table 2 for relevant group averages. Note that the SSCX was not examined further in these thionin-based cytology assessments since differences were not observed following IF analysis and VENs have not been observed in this area.

4 | DISCUSSION

The findings of the current study provide insights into the neurobiological mechanisms of problem-solving abilities in raccoons. Corroborating previous research emphasizing the influence of hippocampal plasticity in altered learning and memory outcomes (Guigueno & Sherry, 2017; Maguire et al., 2006; Sherry & Hoshooley, 2010; Sobrero et al., 2016), hippocampal cellular counts were associated with performance proficiency in the multiaccess problem-solving task. Specifically, the increased number of nonneuronal cells detected in the homogenized hippocampal tissue suggests that glial cells contribute to behavioral outcomes in this particular task. As predicted, no differences in cellular distributions among the three levels of performance were observed in the SSCX. Focusing on neuronal cytoarchitectural profiles in the thionin-stained tissue, the high-solving group had significantly more elongated fusiform cells in the dentate gyrus. Further, the existence of VENs (determined via morphology characteristics) in the FI cortex confirmed previous unpublished evidence of VENs in the raccoon. Differences in VEN counts in the FI, however, were not observed among the three solving groups. To our knowledge, these results represent the first functional neuroanatomical findings associated with cognitive ability in the raccoon.

As evident in their proficiency in obtaining anthropogenic sources of food in urban habitats (Prange et al., 2004), raccoons are known to approach novel challenges in innovative ways (Daniels et al., 2019; Morton, 2020; Stanton et al., 2017). The reported problem-solving flexibility in raccoons may be influenced by their primate-like cortical

neuronal density (Herculano-Houzel et al., 2006; Jardim-Messeder et al., 2017). Raccoons have approximately 400 million cortical neurons, a significant increase from the rat preclinical model that possesses approximately 32 million cortical neurons (Herculano-Houzel, 2009). Considering that humans possess approximately 16 billion cortical neurons (Herculano-Houzel, 2009; Herculano-Houzel, 2012), the complexity of the raccoon's cerebral cortex, coupled with the magnification of the forepaw/hand area, make it an attractive model for translational neuroscience research.

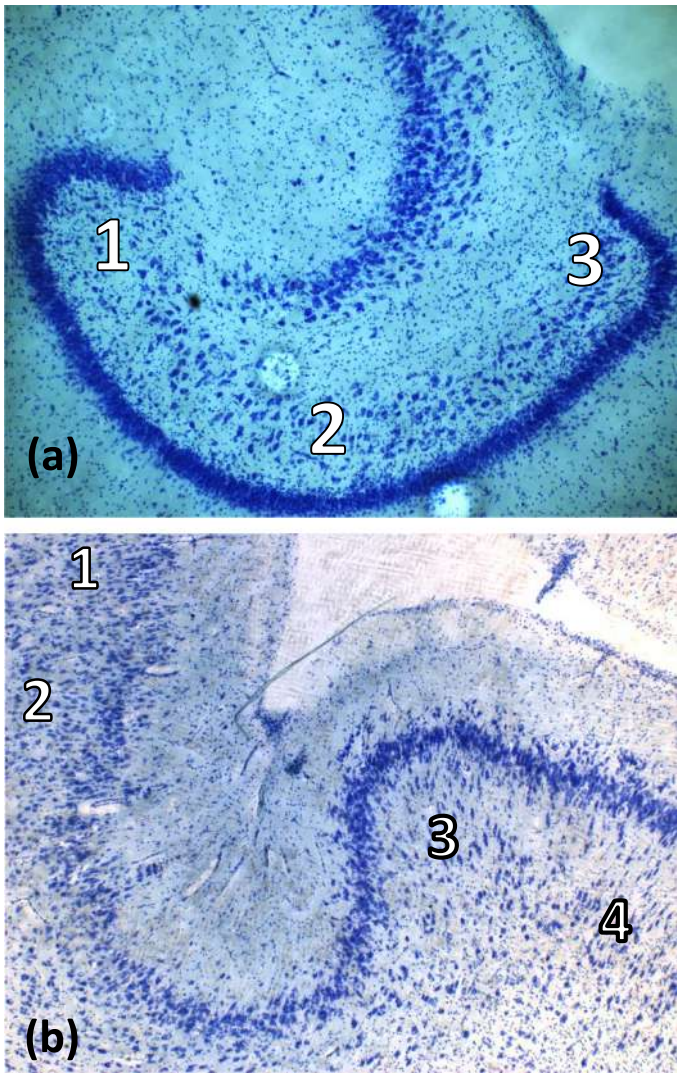

FIGURE 5 Representative images and sampling locations for cell counting in thionin-stained tissue. (a) The dentate gyrus (hilus) of the hippocampus shown at 2.5×, with numbers representing the three sampling regions collected within each tissue section for each animal. (b) The anterior frontoinsular region shown at 5×, with numbers outlining the four general sampling locations for all tissue sections [Color figure can be viewed at wileyonlinelibrary.com]

Focusing on hippocampal cytological parameters determined by IF, the high-performing raccoons possessed a higher number of non-neuronal cells than the lower performing animals. As observed with neurons, glial complexity can contribute to neuroplasticity and adaptive behavioral outcomes (Hoogland & Parpura, 2015). The brain's glial cells, including astrocytes, microglia, and oligodendroglia, differentially contribute to neural functions (Fields et al., 2014). Myelination provided by oligodendroglia facilitate the velocity of neuronal conductance (Nave, 2010); astrocytes regulate local blood flow that facilitates the movement of neurochemicals and nutrients to the neurons (MacVicar & Newman, 2015), and microglia maintain neural circuitry by surveying potential threats and influencing neuroplasticity (Wake et al., 2013). Additional functional roles of astrocytes have been identified in the facilitation of synaptic plasticity and regulation of neuronal network oscillations processes that influence cognitive functions (Santello et al., 2019). Thus, the increased number of glial cells in the hippocampal area of the raccoons may have contributed to the efficient problem-solving ability of the high-performing animals in multiple ways. Caution should be taken when interpreting these findings; however, since specific glial markers were not used in the IF assays. These findings are also limited by task exposure duration considering that the nonsolvers had less time interacting with the puzzle box due to their dismissal from the trials after failing to solve the initial locking task panel. Subsequent investigations controlling for the duration of task interactions would further clarify these initial findings to discern predisposed versus training-induced influences on the hippocampal cellular counts.

Following the report of lower neuronal to glial ratios in specific cortical areas of noted "genius" Albert Einstein, neuron to glia ratios have also been associated with cognitive complexity (Diamond et al., 1985; Tien et al., 2019). Now that it is known that glial cell density varies across different brain areas (Herculano-Houzel, 2014; Herculano-Houzel et al., 2006), it is important to investigate the neuron vs. glial densities to learn more about its contribution to functional output. For example, compared to other primates, a lower neuron to glial ratio is observed in the human frontal cortex (Sherwood et al., 2006). Even so, little evidence of function-related intraspecies

TABLE 2 Cytoarchitecture analysis of sampled regions from the anterior frontoinsular region in raccoons

Solver type	Nonneurons	Neuron total	VENs	Fork neurons	% VENs[a]	% All neurons[b]
Nonsolver ($N = 5$)	88.84 ± 8.17	34.11 ± 3.31	2.30 ± 0.62	0.26 ± 0.13	6.88 ± 1.80	27.75 ± 0.84
Solver ($N = 7$)	74.25 ± 1.96	30.55 ± 1.27	2.82 ± 0.36	0.18 ± 0.08	9.51 ± 1.62	29.12 ± 0.77

Note: Values (mean ± *SEM*) represent averages from the field of vision (200 × 300 μm), and are not cumulative counts.
Abbreviation: VEN, von Economo neuron.
[a]% VEN represents the proportion of neurons characterized as VENs.
[b]% All neurons represent the proportion of total cells that were characterized as VEN, fork, or pyramidal neurons.

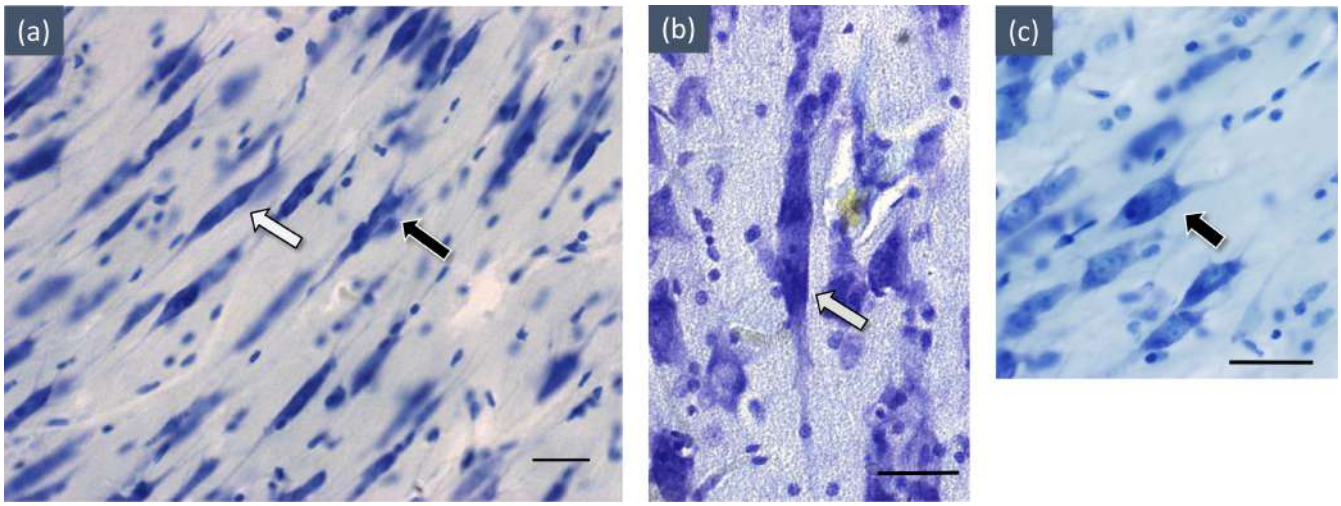

FIGURE 6 Frontoinsular cellular phenotypes. Photomicrographs of thionin-stained cells imaged at 40×, located in the frontoinsular region. Among nonneurons and pyramidal neurons (a), the presence of both von Economo neurons (a,b) and fork neurons (a,c) were observed. White arrows designate von Economo cells, and black arrows designate fork cells. All scale bars represent 30 μm. A summary of all other cellular profiling measures can be found in Table 2 [Color figure can be viewed at wileyonlinelibrary.com]

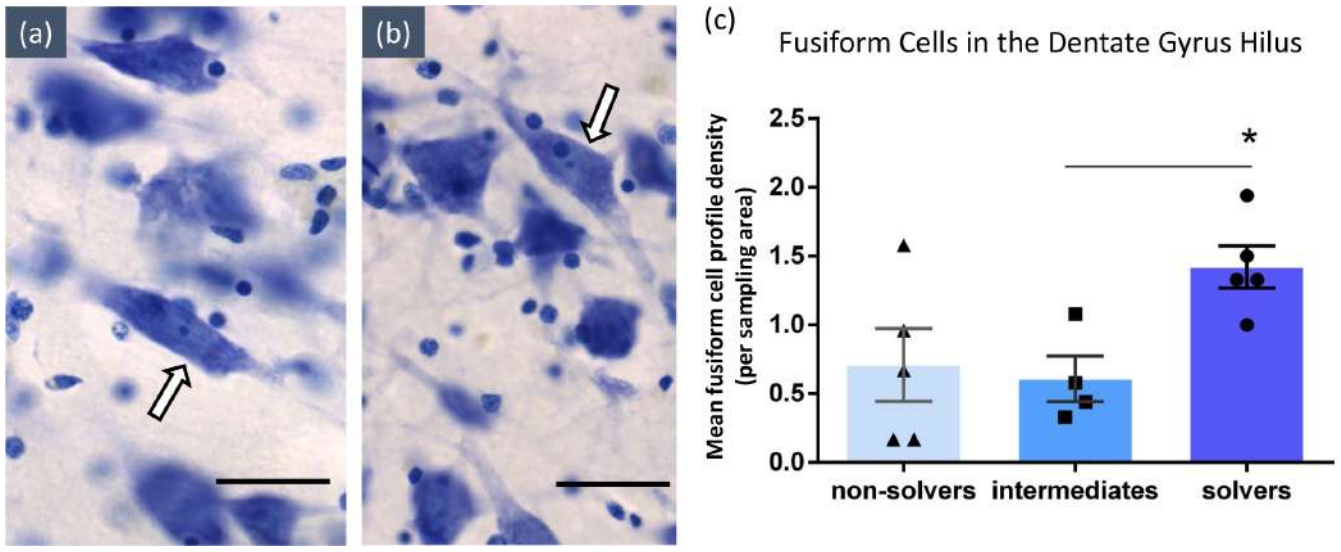

FIGURE 7 Fusiform cells in the raccoon dentate gyrus hilus. Representative photomicrographs of thionin-stained fusiform cells observed in the hilus at 40× (a,b). These cells were found to be more prevalent in high-problem solving raccoons, compared to intermediate or nonsolving raccoons (c). Significant differences were detected between solvers and intermediates via a one-way analysis of variance (ANOVA), with Tukey's post hoc (*$p = .0495$). All other cell-profiling measures for the hippocampus cells can be found in Table 3. All scale bars represent 30 μm [Color figure can be viewed at wileyonlinelibrary.com]

neuron to glia ratio differences have been observed in preclinical models (Bardi et al., 2016). Although no differences in percentages of neurons in sampled areas were observed in the hippocampal hilus or FI area in the current study, it is important to continue to investigate these cellular profiles in functional neuroscience explorations. Considering that the use of thionin-based morphology to identify nonneuronal cells such as glial cells (García-Cabezas et al., 2016) is less reliable than more specific cellular profiling (e.g., neurochemical or transcriptomic markers) and stereological-based estimations, additional histological analyses would be informative.

Described as homologous to extratelencephalic excitatory projecting neurons (Hodge et al., 2020), VENs may facilitate the rapid processing of neural information in targeted brain areas (Hakeem et al., 2009; Stimpson et al., 2011). In the neuron-dense human cortex, the *connectomic hypothesis* suggests that the presence of VENs leads to more rapid cellular projections among specialized neural modules that facilitate sustained neural activation for advanced cognitive

TABLE 3 Cytoarchitecture analysis of the hilus of the dentate gyrus region in raccoons

Solver type	Nonneurons	Neuron total	Fusiform neurons	% Fusiform neurons[a]	% All neurons[b]
Nonsolver ($N = 5$)	120.0 ± 9.15	27.80 ± 3.41	0.71 ± 0.27	2.73 ± 0.52	18.74 ± 1.73
Intermediate ($N = 4$)	119.05 ± 5.17	27.09 ± 1.99	0.61 ± 0.17	2.31 ± 0.65	18.64 ± 1.43
Solver ($N = 5$)	105.6 ± 9.99	29.60 ± 4.61	1.42 ± 0.15*	5.08 ± 0.61	21.93 ± 3.06

Note: Values (mean ± *SEM*) represent averages from the field of vision (200 × 300 μm), and are not cumulative counts.
[a]% Fusiform neurons represent the proportion of neurons characterized as fusiform cells.
[b]% Neurons represents the proportion of total cells that were characterized as either fusiform cells or other neurons.

functions—a neural model also referred to as the *global neuronal workspace* (Mashour et al., 2020). Although no differences in number of VENs in the FI were observed among the three groups of raccoons, once again, VENs were confirmed to be present in the FI cortex. Considering the absence of these neurons in rodent models, this finding provides further support for the translational value of the raccoon model. Even in the absence of differential contributions of VENs to problem-solving ability, their presence provides potential insights into the cognitive abilities of raccoons. For example, the postnatal emergence of VENs suggests that an animal's experiences, broadly defined, influence VEN development (Allman et al., 2011), providing evidence of their putative role in the formation of specialized neural circuits that facilitate an animal's unique and adaptive behavioral responses (Stimpson et al., 2011). Further, the fourfold increase of VENs in "super-agers" who show little evidence of age-typical cognitive decline provides evidence of the potential facilitatory role of VENs in cognitive functions (Rogalski et al., 2013). Additionally, the increased density of VENS in the crest, as opposed to the walls, in the human medial frontopolar cortex suggests that VENs may also serve a mechanical function in cortical gyrification (Gonzalez-Acosta et al., 2018).

Considering the similarity between the morphology of VENs and bipolar fusiform cells, it is interesting that more fusiform cells were observed in the dentate gyrus of the high-performing raccoons. Individual differences in dentate gyrus cell numbers were also observed in degus (*Octodon degus*), suggesting that this area is likely responsive to individual environmental and social experiences (Sobrero et al., 2016). Additionally, bipolar fusiform cells increase processing speed within the HC and extrahippocampal areas in a similar, but less rapid, fashion as the cortical VENs (Scharfman, 2011; Schwerdtfeger & Buhl, 1986). In the absence of VENs in the ACC (as observed in previously unpublished findings in our laboratory), these subcortical fusiform cells may facilitate emotional and cognitive processing in the raccoon. Interestingly, VENs were also observed to be scarce in the elephant ACC, providing additional evidence that the cortical landscape of VENs has evolved independently for species-specific adaptive functions (Hakeem et al., 2009). For example, the existence of VENs in the posterior insular cortex may enhance transmission of auditory and visceral autonomic functions leading to increased survival in prey species that have VENs, such as deer and sheep (Raghanti et al., 2015). The rich network of interoceptive afferents in the macaque insular cortex that facilitates the perceived physiological status of the body's organs provides additional support for the VENs in visceral functions (Evrard, 2019). Further, VEN expression of FE2FZ and CTIP2, transcription factors known to regulate subcerebral projections, likely facilitate the linkage of cortical autonomic target sites to downstream brainstem and spinal cord sites (Cobos & Seeley, 2015). Thus, compared to species with VENs in both the FI and ACC, unique VEN distributions in the raccoon may result in varied functional outcomes; consequently, the specific distribution patterns on VENS should be more thoroughly investigated.

The convergence of findings in the current study suggests that the raccoon model is valuable for neuroscience research. Although housing raccoons in traditional laboratories is not a practical option, it is important to explore various field techniques that provide relevant neurobiological data in a diverse array of species to contribute to the growing body of rodent neurobiological findings. For example, the IF technique provides an opportunity to investigate intraspecies cellular densities in post-fixed tissue extracted from wild-caught animals. Such investigations will increase our knowledge of functional neuroscience influences (e.g., cellular profiles of animals with varying cognitive abilities) in animals living inside and outside of laboratory conditions. Further, the presence of VENs in the raccoon FI offers an opportunity to explore how these rapidly processing neurons facilitate complex cognitive functions. Considering that alterations in VEN populations have been associated with several neuropsychiatric conditions including autism, schizophrenia, and dementia (Allman et al., 2005; Cauda et al., 2014; Seeley et al., 2006), the translational value of preclinical models that possess these neuron types increases the likelihood of identifying key mechanisms of these challenging and threatening conditions. Additional research confirming the role of varied cytoarchitectural landscapes on behavioral outcomes will contribute valuable information to emerging neuroethological and psychiatric knowledge bases.

ACKNOWLEDGMENTS

The authors appreciate the support of the University of Richmond Psychology Department and the Arts and Sciences Summer Fellowship Program at the University of Richmond as well as the Schapiro Undergraduate Summer Research Fellowship program at Randolph-Macon College. No external funds were used to support this research.

AUTHOR CONTRIBUTIONS

Joanna Jacob, **Molly Kent**, and **Kelly Lambert**: Participated in data collection, data analysis, and manuscript preparation. **Sarah Benson-Amram**, **Suzana Herculano-Houzel**, and **Mary Ann Raghanti**:

Participated in data collection and manuscript preparation. **Emily Ploppert**, **Jack Drake**, **Bilal Hindi**, **Nick R. Natale**, **Sarah Daniels**, **Rachel Fanelli**, **Anderson Miller**, **Tim Landis**, **Amy Gilbert**, **Shylo Johnson**, **Annie Lai**, **Molly Hyer**, **Amanda Rzucidlo**, **Chris Anchor**, and **Stan Gehrt**: Participated in data collection.

PEER REVIEW

The peer review history for this article is available at https://publons.com/publon/10.1002/cne.25197.

DATA AVAILABILITY STATEMENT

Raw data included in this manuscript were generated at the University of Richmond and are available from the corresponding author (K. L.) upon request.

ORCID

Suzana Herculano-Houzel https://orcid.org/0000-0002-1765-3599
Kelly Lambert https://orcid.org/0000-0003-1626-5129

REFERENCES

Allman, J. M., Tetreault, N. A., Hakeem, A. Y., Manaye, K. F., Semendeferi, K., Erwin, J. M., Park, S., Goubert, V., & Hof, P. R. (2010). The von Economo neurons in frontoinsular and anterior cingulate cortex in great apes and humans. *Brain Structure & Function*, *214*, 495–517. https://doi.org/10.1007/s00429-010-0254-0

Allman, J. M., Tetreault, N. A., Hakeem, A. Y., & Park, S. (2011). The von Economo neurons in apes and humans. *American Journal of Human Biology*, *23*(1), 5–21. https://doi.org/10.1002/ajhb.21136

Allman, J. M., Watson, K. K., Tetreault, N. A., & Hakeem, A. Y. (2005). Intuition and autism: A possible role for von Economo neurons. *Trends in Cognitive Sciences*, *9*(8), 367–373.

Bandeira, F., Lent, R., & Herculano-Houzel, S. (2009). Changing numbers of neuronal and non-neuronal cells underlie postnatal brain growth in the rat. *Proceedings of the National Academy of Sciences of the United States of America*, *106*(33), 14108–14113. https://doi.org/10.1073/pnas.0804650106

Bardi, M., Kaufman, C., Franssen, C., Hyer, M. M., Rzucidlo, A., Brown, M., Tschirhart, M., & Lambert, K. G. (2016). Paper or plastic? Exploring the effects of natural enrichment on Behavioural and neuroendocrine responses in long-Evans rats. *Journal of Neuroendocrinology*, *28*(5). https://doi.org/10.1111/jne.12383

Benes, F. M., & Lange, N. (2001). Two-dimensional versus three-dimensional cell counting: a practical perspective. *Trends in Neurosciences*, *24*(1), 11–17. https://doi.org/10.1016/s0166-2236(00)01660-x

Bird, C. M., & Burgess, N. (2008). The hippocampus and memory: Insights from spatial processing. *Nature Reviews. Neuroscience*, *9*(3), 182–194.

Butti, C., Fordyce, E. R., Raghanti, M. A., Gu, X., Bonar, C. J., Wicinski, B. A., Wong, E. W., Roman, J., Brake, A., Eaves, E., Spocter, M. A., Tang, C. Y., Jacobs, B., Sherwood, C. C., & Hof, P. R. (2014). The cerebral cortex of the pygmy hippopotamus, *Hexaprotodon liberiensis* (Cetartiodactyla, Hippopotamidae): MRI, cytoarchitecture, and neuronal morphology. *Anatomical Record (Hoboken)*, *297*(4), 670–700. https://doi.org/10.1002/ar.22875

Butti, C., Janeway, C. M., Townshend, C., Wicinski, B. A., Reidenberg, J. S., Ridgway, S. H., Sherwood, C. C., Hof, P. R., & Jacobs, B. (2015). The neocortex of cetartiodactyls: I. A comparative golge analysis of neuronal morphology in the bottlenose dolphin (Tursiops truncates), the minke whale (*Balaenoptera acutorostrata*), and the humpback whale (*Megaptera novaeangliae*). *Brain Structure & Function*, *22*, 3339–3368.

Butti, C., Sanos, M., Uppal, N., & Hof, P. R. (2013). Von Economo neurons: Clinical and evolutionary perspectives. *Cortex*, *49*(1), 312–326.

Cauda, F., Geminiani, G. C., & Vercelli, A. (2014). Evolutionary appearance of von Economo's neurons in the mammalian cerebral cortex. *Frontiers in Human Neuroscience*, *8*, 104. https://doi.org/10.3389/fnhum.2014.00104

Citri, A., & Malenka, R. (2008). Synaptic plasticity: Multiple forms, functions, and mechanisms. *Neuropsychopharmacol*, *33*, 18–41. https://doi.org/10.1038/sj.npp.1301559.

Cobos, I., & Seeley, W. W. (2015). Human von Economo neurons express transcription factors associated with layer V subcerebral projection neurons. *Cerebral Cortex*, *25*(1), 213–220. https://doi.org/10.1093/cercor/bht219

Cole, L. W. (1907). Concerning the intelligence of raccoons. *Journal of Comparative Neurology and Psychology*, *17*, 211–261.

Correa-Júnior, N. D., Renner, J., Fuentealba-Villarroel, F., Hilbig, A., & Rasia-Filho, A. A. (2020). Dendritic and spine heterogeneity of von Economo neurons in the human cingulate cortex. *Frontiers in Synaptic Neuroscience*, *12*(12), 25. https://doi.org/10.3389/fnsyn.2020.00025

Dallérac, G., & Rouach, N. (2016). Astrocytes as new targets to improve cognitive functions. *Progress in Neurobiology*, *144*, 48–67. https://doi.org/10.1016/j.pneurobio.2016.01.003

Daniels, S. E., Fanelli, R. E., Gilbert, A., & Benson-Amram, S. (2019). Behavioral flexibility of a generalist carnivore. *Animal Cognition*, *22*(3), 387–396.

Davis, H. B. (1907). The raccoon: A study in animal intelligence. *The American Journal of Psychology*, *18*(4), 447–489.

Denayer, T., Stöhr, T., & van Roy, M. (2014). Animal models in translational medicine: Validation and prediction. *New Horizons in Translational Medicine*, *2*(1), 5–11.

Diamond, M. C., Scheibel, A. B., Murphy, G. M., Jr., & Harvey, T. (1985). On the brain of a scientist: Albert Einstein. *Experimental Neurology*, *88*(1), 198–204.

Dickerson, B. C., Miller, S. L., Greve, D. N., Dale, A. M., Albert, M. S., Schacter, D. L., & Sperling, R. A. (2007). Prefrontal-hippocampal-fusiform activity during encoding predicts intraindividual differences in free recall ability: an event-related functional-anatomic MRI study. *Hippocampus*, *17*(11), 1060–1070. https://doi.org/10.1002/hipo.20338.

Dijkstra, A. A., Lin, L.-C., Nana, A. L., Gaus, S. E., & Seeley, W. W. (2018). Von Economo neurons and fork cells: A neurochemical signature linked to monoaminergic function. *Cerebral Cortex*, *28*(1), 131–144. https://doi.org/10.1093/cercor/bhw358

Evrard, H. C. (2019). The organization of the primate insular cortex. *Frontiers in Neuroanatomy*, *13*, 43. https://doi.org/10.3390/franca.2019.0043

Evrard, H. C., Forro, T., & Logothetis, N. K. (2012). Von Economo neurons in the anterior insula of the macaque monkey. *Neuron*, *74*(3), 482–489. https://doi.org/10.1016/j.neuron.2012.03.003

Fields, R. D., Araque, A., Johansen-Berg, H., Lim, S.-S., Lynch, G., Nave, K.-A., Nedergaard, M., Perez, R., Sejnowski, T., & Wake, H. (2014). Glial biology in learning and cognition. *The Neuroscientist*, *20*(5), 426–431.

García-Cabezas, M. Á., John, Y. J., Barbas, H., & Zikopoulos, B. (2016). Distinction of neurons, glia and endothelial cells in the cerebral cortex: An algorithm based on cytological features. *Frontiers in Neuroanatomy*, *10*, 107. https://doi.org/10.3389/fnana.2016.00107

Gienapp, P., Teplitsky, C., Alho, J. S., Mills, J. A., & Merilä, J. (2008). Climate change and evolution: Disentangling environmental and genetic responses. *Molecular Ecology*, *17*(1), 167–178.

Gonzalez-Acosta, C. A., Escobar, M. I., Casanova, M. F., Pimienta, H. J., & Buritica, E. (2018). Von Economo neurons in the human medial frontopolar cortex. *Frontiers in Neuroanatomy*, *12*, 64. https://doi.org/10.3389/fnana.2018.00064

Guigueno, M. F., & Sherry, D. F. (2017). Hippocampus and spatial memory in brood parasitic cowbirds. M. Soler (ed.), *Avian Brood Parasitism*,

Fascinating Life Sciences, (Chp. 11, pp. 203–218). Springer International Publishing AG, part of Springer Nature 2017. https://doi.org/10.1007/978-3-319-73138-4_11

Hakeem, A. Y., Sherwood, C. C., Bonar, C. J., Butti, C., Hof, P. R., & Allman, J. M. (2009). Von Economo neurons in the elephant brain. *The Anatomical Record: Advances in Integrative Anatomy and Evolutionary Biology*, *292*(2), 242–248. https://doi.org/10.1002/ar.20829

Hamir, A. N. (2011). Pathology of neurologic disorders of raccoons (*Procyon lotor*). *Journal of Veterinary Diagnostic Investigation*, *23*(5), 873–884.

Hartley, T., Bird, C. M., Chan, D., Cipolotti, L., Husain, M., Vargha-Khadem, F., & Burgess, N. (2007). The hippocampus is required for short-term topographical memory in humans. *Hippocampus*, *17*(1), 34–48. https://doi.org/10.1002/hipo.20240

Herculano-Houzel, S. (2009). The human brain in numbers: A scaled-up primate brain. *Frontiers in Human Neuroscience*, *3*, 31. https://www.ncbi.nlm.nih.gov/pmc/articles/PMC2776484/

Herculano-Houzel, S. (2011). Scaling of brain metabolism with a fixed energy budget per neuron: Implications for neuronal activity, plasticity and evolution. *PLoS One*, *6*(3), e17514. https://doi.org/10.1371/journal.pone.0017514

Herculano-Houzel, S. (2012). The not so extraordinary human brain. Proceedings of the National Academy of Sciences, 109, 10661–10668. https://doi.org/10.1073/pnas.1201895109

Herculano-Houzel, S. (2014). The glia/neuron ratio: How it varies uniformly across brain structures and species and what that means for brain physiology and evolution. *Glia*, *62*(9), 1377–1391.

Herculano-Houzel, S., & Lent, R. (2005). Isotropic fractionator: A simple, rapid method for the quantification of total cell and neuron numbers in the brain. *The Journal of Neuroscience*, *25*(10), 2518–2521.

Herculano-Houzel, S., Mota, B., & Lent, R. (2006). Cellular scaling rules for rodent brains. *Proceedings of the National Academy of Sciences of the United States of America*, *103*(32), 12138–12143.

Herron, P. (1978). Somatotopic organization of mechanosensory projections to SII cerebral neocortex in the raccoon (*Procyon lotor*). *The Journal of Comparative Neurology*, *181*, 717–727. https://doi.org/10.1002/cne.901810403

Hirsch, B. T., Prange, S., Hauver, S. A., & Gehrt, S. D. (2013). Raccoon social networks and the potential for disease transmission. *PLoS One*, *8*(10), e75830.

Hodge, R., Miller, J., Novotny, M., Ting, J., Kalmbach, B., Bakken, T., Aevermann, B., Barkan, E., Berkowitz-Cerasano, M., Cobbs, C., Diez-Fuertes, F., Ding, S.-L., Mccorrison, J., Schork, N., Shehata, S., Smith, K., Sunkin, S., Tran, D., Venepally, P., … Lein, E. (2020). Transcriptomic evidence that von Economo neurons are regionally specialized extratelencephalic-projecting excitatory neurons. *Nature Communications*, *11*, 1172. https://www.nature.com/articles/s41467-020-14952-3

Hof, P. R., & van der Gucht, E. (2007). Structure of the cerebral cortex of the humpback whale, *Megaptera novaeangliae* (Cetacea, Mysticeti, Balaenopteridae). *Anatomical Record*, *290*, 1–31. https://doi.org/10.1002/ar.20407

Hoogland, T. M., & Parpura, V. (2015). The role of glia in plasticity and behavior. *Frontiers in Cellular Neuroscience*, *9*, 356.

Hunter, W. S. (1913). The delayed reaction in animals and children. https://doi.org/10.5962/bhl.title.45847

Hunter, W. S. (1915). A reply to some criticisms of the delayed reaction. *The Journal of Philosophy, Psychology and Scientific Methods*, *12*(2), 38–41.

Ibegbu, A., Umana, U., Hamman, O., & Adamu, S. (2015). Von Economo neurons: A review of the anatomy and functions. *Journal of Experimental and Clinical Anatomy*, *14*(2), 126–130. https://doi.org/10.4103/1596-2393.177023

Iwaniuk, A. N., & Whishaw, I. Q. (1999). How skilled are the skilled limb movements of the raccoon (*Procyon lotor*)? *Behavioural Brain Research*, *99*(1), 35–44.

Jardim-Messeder, D., Lambert, K., Noctor, S., Pestana, F. M., de Castro Leal, M. E., Bertelsen, M. F., Alagaili, A. N., Mohammad, O. B., Manger, P. R., & Herculano-Houzel, S. (2017). Dogs have the most neurons, though not the largest brain: Trade-off between body mass and number of neurons in the cerebral cortex of large Carnivoran species. *Frontiers in Neuroanatomy*, *11*, 118. https://doi.org/10.3389/fnana.2017.00118

Kempermann, G. (2002). Neuronal stem cells and adult neurogenesis. *Ernst Schering Research Foundation workshop*, (35), 17–28. https://doi.org/10.1007/978-3-662-04816-0_2

Kempermann, G. (2012). New neurons for the 'survival of the fittest'. *Nature Reviews Neuroscience*, *13*, 727–736.

Kempermann, G., & Gage, F. H. (1999). Experience-dependent regulation of adult hippocampal neurogenesis: effects of long-term stimulation and stimulus withdrawal. *Hippocampus*, *9*(3), 321–332. https://doi.org/10.1002/(SICI)1098-1063(1999)9:3<321::AID-HIPO11>3.0.CO;2-C.

Krebs, J. R., Sherry, D. F., Healy, S. D., Perry, V. H., & Vaccarino, A. L. (1989). Hippocampal specialization of food-storing birds. *Proceedings of the National Academy of Sciences of the United States of America*, *86*, 1388–1381.

Krubitzer, L. (2007). The magnificent compromise: Cortical field evolution in mammals. *Neuron*, *56*(2), 201–208. https://doi.org/10.1016/j.neuron.2007.10.002

Krubitzer, L., & Dooley, J. C. (2013). Cortical plasticity within and across lifetimes: How can development inform us about phenotypic transformations? *Frontiers in Human Neuroscience*, *7*, 620. https://doi.org/10.3389/fnhum.2013.00620

Lambert, K., Kent, M., & Vavra, D. (2019). Avoiding Beach's Boojum effect: Enhancing bench to bedside translation with field to laboratory considerations in optimal animal models. *Neuroscience and Biobehavioral Reviews*, *104*, 191–196.

Luo, J., & Niki, K. (2003). Function of hippocampus in "insight" of problem-solving. *Hippocampus*, *13*, 316–323.

Lynch, G., Gall, C., & Dunwiddie, T. V. (1978). Neuroplasticity in the hippocampal formation. *Progress in Brain Research*, *48*, 113–130.

MacClintock, D. (2002). *A natural history of raccoons*. Blackburn Press.

MacVicar, B. A., & Newman, E. A. (2015). Astrocyte regulation of blood flow in the brain. *Cold Spring Harbor Perspectives in Biology*, *7*(5), a020388. https://doi.org/10.1101/cshperspect.a020388

Maguire, E. A., Spiers, H. J., Good, C. D., Hartley, T., Frackowiak, R. S. J., & Burgess, N. (2003). Navigation expertise and the human hippocampus: A structural brain imaging analysis. *Hippocampus*, *13*(2), 250–259.

Maguire, E. A., Woollett, K., & Spiers, H. J. (2006). London taxi drivers and bus drivers: A structural MRI and neuropsychological analysis. *Hippocampus*, *16*(12), 1091–1101.

Mashour, G. A., Roelfsema, P., Changeux, J.-P., & Dehaene, S. (2020). Conscious processing and the global neuronal workspace hypothesis. *Neuron*, *105*(5), 776–798. https://doi.org/10.1016/j.neuron.2020.01.026

Morton, F. B. (2020). Do wild raccoons (*Procyon lotor*) use tools? *Animal Cognition*, *24*, 433–441. https://doi.org/10.1007/s10071-020-01430-y

Myers, C. E., & Scharfman, H. E. (2009). A role for hilar cells in pattern separation in the dentate gyrus: A computational approach. *Hippocampus*, *19*, 321–337.

Nave, K.-A. (2010). Myelination and support of axonal integrity by glia. *Nature*, *468*(7321), 244–252.

Nimchinsky, E. A., Gilissen, E., Allman, J. M., Perl, D. P., Erwin, J. M., & Hof, P. R. (1999). A neuronal morphologic type unique to humans and great apes. *Proceedings of the National Academy of Sciences of the United States of America*, *96*(9), 5268–5273. https://doi.org/10.1073/pnas.96.9.5268

Nimchinsky, E. A., Vogt, B. A., Morrison, J. H., & Hof, P. R. (1995). Spindle neurons of the human anterior cingulate cortex. *Journal of Comparative Neurology*, *355*(1), 27–37. https://doi.org/10.1002/cne.903550106

Pettit, M. (2010). The problem of raccoon intelligence in behaviourist America. *British Journal for the History of Science*, *43*(3), 391–421.

Poskanzer, K. E., & Yuste, R. (2016). Astrocytes regulate cortical state switching in vivo. *Proceedings of the National Academy of Sciences of the United States of America*, *113*(19), E2675–E2684. https://doi.org/10.1073/pnas.1520759113

Prange, S., Gehrt, S. D., & Wiggers, E. P. (2004). Influences of anthropogenic resources on raccoon (*Procyon lotor*) movements and spatial distribution. *Journal of Mammalogy*, *85*(3), 483–490.

Pravosudov, V. V., & Clayton, N. S. (2002). A test of the adaptive specialization hypothesis: Population differences in caching, memory, and the hippocampus in black-capped chickadees (*Poecile atricapillus*). *Behavioral Neuroscience*, *116*(4), 515–522. https://doi.org/10.1037/0735-7044.116.4.515

Pubols, B. H., Welker, W. I., & Johnson, J. I. (1965). Somatic sensory representation of forelimb in dorsal root fibers of raccoon, coatimundi, and cat. *Journal of Neurophysiology*, *28*(2), 312–341. https://doi.org/10.1152/jn.1965.28.2.312

Raghanti, M. A., Spurlock, L. B., Treichler, F. R., Weigel, S. E., Stimmelmayr, R., Butti, C., Thewissen, J. G. M. H., & Hof, P. R. (2015). An analysis of von Economo neurons in the cerebral cortex of cetaceans, artiodactyls, and perissodactyls. *Brain Structure & Function*, *220*(4), 2303–2314.

Raghanti, M. A., Wicinski, B., Meierovich, R., Warda, T., Dickstein, D. L., Reidenberg, J. S., Tang, C. Y., George, J. C., Hans Thewissen, J., Butti, C., & Hof, P. R. (2019). A comparison of the cortical structure of the bowhead whale (*Balaena mysticetus*), a basal mysticete, with other cetaceans. *The Anatomical Record*, *302*, 745–760. https://doi.org/10.1002/ar.23991

Rogalski, E. J., Gefen, T., Shi, J., Samimi, M., Bigio, E., Weintraub, S., Geula, C., & Mesulam, M. M. (2013). Youthful memory capacity in old brains: Anatomic and genetic clues from the Northwestern SuperAging Project. *Journal of Cognitive Neuroscience*, *25*(1), 29–36. https://doi.org/10.1162/jocn_a_00300

Santello, M., Toni, N., & Volterra, A. (2019). Astrocyte function from information processing to cognition and cognitive impairment. *Nature Neuroscience*, *22*(2), 154–166. https://doi.org/10.1038/s41593-018-0325-8

Scharfman, H. E. (2011). *The dentate gyrus: A comprehensive guide to structure, function, and clinical implications*. Elsevier.

Schober, W. (1991). The brain of the raccoon (Procyon lotor) in stereotactic coordinates. *Journal fur Hirnforschung*, *32*, 665–686.

Schwerdtfeger, W. K., & Buhl, E. (1986). Various types of non-pyramidal hippocampal neurons project to the septum and contralateral hippocampus. *Brain Research*, *386*(1,2), 146–154. https://doi.org/10.1016/0006-8993(86)90151-4

Seeley, W. W., Carlin, D. A., Allman, J. M., Macedo, M. N., Bush, C., Miller, B. L., & Dearmond, S. J. (2006). Early frontotemporal dementia targets neurons unique to apes and humans. *Annals of Neurology*, *60*(6), 660–667.

Sherry, D. F., & Hoshooley, J. S. (2010). Seasonal hippocampal plasticity in food-storing birds. *Philosophical Transactions of the Royal Society of London. Series B, Biological Sciences*, *365*(1542), 933–943.

Sherwood, C. C., Stimpson, C. D., Raghanti, M. A., Wildman, D. E., Uddin, M., Grossman, L. I., Goodman, M., Redmond, J. C., Bonar, C. J., Erwin, J. M., & Hof, P. R. (2006). Evolution of increased glia-neuron ratios in the human frontal cortex. *Proceedings of the National Academy of Sciences of the United States of America*, *103*(37), 13606–13611.

Shubha, S., & Suchi, S. (2017). Von Economo neurons in Indian green ring neck parrot (*Psittacula krameri*): Possible role in vocal learning. *Austin Journal of Anatomy*, *4*(3), 1072. https://doi.org/10.26420/austinjanat.2017.1072

Sobrero, R., Fernández-Aburto, P., Ly-Prieto, Á., Delgado, S. E., Mpodozis, J., & Ebensperger, L. A. (2016). Effects of habitat and social complexity on brain size, brain asymmetry and dentate gyrus morphology in two octodontid rodents. *Brain, Behavior and Evolution*, *87*(1), 51–64.

Stanton, L. A., Bridge, E. S., Huizinga, J., Johnson, S. R., Youngo, J. K., & Benson-Amran, S. (2020). Variation in reversal learning by three generalist mesocarnivores. *Animal Cognition*, *24*, 555–568. https://doi.org/10.1007/s10071-020-01438-4

Stanton, L., Davis, E., Johnson, S., Gilbert, A., & Benson-Amram, S. (2017). Adaptation of the Aesop's Fable paradigm for use with raccoons (Procyon lotor): Considerations for future application in non-avian and non-primate species. *Animal Cognition*, *20*(6), 1147–1152. https://doi.org/10.1007/s10071-017-1129-z.

Stimpson, C. D., Tetreault, N. A., Allman, J. M., Jacobs, B., Butti, C., Hof, P. R., & Sherwood, C. C. (2011). Biochemical specificity of von Economo neurons in hominoids. *American Journal of Human Biology*, *23*(1), 22–28.

Tien, T. S., van Hung, N., Tuan, N. T., van Nam, N., An, N. Q., Minh Thuy, N. T., Kim Lien, V. T., & van Nghia, N. (2019). High-order EXAFS cumulants of diamond crystals based on a classical anharmonic correlated Einstein model. *The Journal of Physics and Chemistry of Solids*, *134*, 307–312.

Tyng, C. M., Amin, H. U., Saad, M. N. M., & Malik, A. S. (2017). The influences of emotion on learning and memory. *Frontiers in Psychology*, *8*. https://doi.org/10.3389/fpsyg.2017.01454

Vasile, F., Dussi, E., & Rouach, N. (2017). Human astrocytes: Structure and function in the healthy brain. *Brain Structure and Function*, *222*, 2017–2019.

von Economo, C. (1926). Eine neue art spezialzellen des lobus cinguli und lobus insulae. *Zschr ges Neurol Psychiat*, *100*, 706–712.

Wake, H., Moorhouse, A. J., Miyamoto, A., & Nabekura, J. (2013). Microglia: Actively surveying and shaping neuronal circuit structure and function. *Trends in Neurosciences*, *36*(4), 209–217.

Welker, W. I., & Seidenstein, S. (1959). Somatic sensory representation in the cerebral cortex of the raccoon (*Procyon lotor*). *The Journal of Comparative Neurology*, *111*, 469–501. https://doi.org/10.1002/cne.901110306

Yassa, M. A., & Stark, C. E. (2011). Pattern separation in the hippocampus. *Trends in Neurosciences*, *34*(10), 515–525. https://doi.org/10.1016/j.tins.2011.06.006

Zeveloff, S. I. (2002). *Raccoons: A natural history*. UBC Press.

How to cite this article: Jacob, J., Kent, M., Benson-Amram, S., Herculano-Houzel, S., Raghanti, M. A., Ploppert, E., Drake, J., Hindi, B., Natale, N. R., Daniels, S., Fanelli, R., Miller, A., Landis, T., Gilbert, A., Johnson, S., Lai, A., Hyer, M., Rzucidlo, A., Anchor, C., Gehrt, S., & Lambert, K. (2021). Cytoarchitectural characteristics associated with cognitive flexibility in raccoons. *Journal of Comparative Neurology*, *529*(14), 3375–3388. https://doi.org/10.1002/cne.25197